Charge Symmetric Background Study

For ^{1}H and ^{2}H Inclusive Cross-section Measurement and F_2 Structure Function Extraction

Progress Report

at Virginia Tech.
at the Department of Physics
PArtonic Structure of the HAdrons (PASHA)

Principal Supervisor:	Prof. Marie Boer
Associate Supervisor:	Dr. Henry Williams
Author:	Gyang Chung 850 W Campus Dr 24061 Blacksburg gyangchung@vt.edu
Submission:	13th July 2023

Abstract

This report gives the findings of work done on charge symmetric background analysis for the extraction of an F_2 function. The F_2 function is a nuclear structure function that is a function of the Bjorken scaling parameter x and the momentum transfer square Q^2. Its determination is important for constraining Parton Distribution Functions (PDFs), parametrizing nuclear scattering reactions within the resonance and Deep Inelastic Scattering (DIS) region, Quark Hadron Duality investigations, proof of lattice QCD and other applications. It is determined through experiments by measuring the inclusive scattering cross-section. The goal is to use an inclusive scattering reaction to obtain F_2 function values for ^{1}H and ^{2}H at the resonance and DIS region for a wide range of x (0.2 to $\approx$1) and Q^2 (4 to 16GeV). The charge symmetric background study is a step toward that goal. Data from the E12-10-002 experiment done at Jefferson Lab. in February and March 2018 were analyzed to acquire two essential parameters that are important for measuring the amount of electrons identified from charge symmetric processes. These parameters were determined for the Hydrogen and Deuterium target for SHMS spectrometer angle of 21^0, 29^0 and 39^0.

Contents

Figures III
1 Introduction 1
2 Background 2
2.1 Introduction 2
2.2 F_2 Nuclear Structure Function 3
3 Analysis 4
3.1 Introduction 4
3.1.1 Charge Symmetric (CS) Processes 4
3.2 CSB Analysis 5
3.3 $\frac{e^+}{e^- - e^+}$ Extraction From the Data 5
3.4 Corrections on Data 6
3.5 $\frac{e^+}{e^- - e^+}$ for SHMS Data 7
4 Conclusion 10
4.1 Conclusion 10
4.2 Future work 10
References IV

Figures

1 First order Feynman diagram for electron-nucleon inclusive scattering, with SHMS detector collecting data of the scattered electron. 2
2 Positive, neutral, and negative Pions constituent quarks. Neutral Pion decay channels and branching ratio. 4
3 Positron Charged Normalized Yield for Hydrogen at 29^0. 6
4 Electron Charged Normalized Yield for Hydrogen at 29^0. 6
5 Histogram of $\frac{e^+}{e^- - e^+}$: corrections placed separately to visualize their effects. 7
6 Histogram of $\frac{e^+}{e^- - e^+}$: corrections added sequentially to visualize their effects. 7
7 Plot of $\frac{e^+}{e^- - e^+}$ as a function of scattered electron energy for different angles. It's more at higher angles 8
8 Positron cross-section. Compared with results from James Madison University (JMU) 8
9 Positron cross-section fitting parameters values with the relative % error 9
10 Percentage error of fitting parameters relative to that from JMU 9

1 Introduction

An inclusive nuclear reaction experiment was conducted in Hall C in 2018 with the aim of measuring the ^{1}H and ^{2}H cross-section and extraction of the F_2 value. Some physics motivation for performing this cross-section of ^{1}H and ^{2}H experiment is to obtain results that will lead to:

- Constraining Parton Distribution Functions (PDFs) within the x and Q^2 for this experiment. This experiment will provide PDF results in some regions of x and Q^2 that are not available in the global data [1], [2].
- A means of providing a better parametrization of the inclusive nuclear scattering reactions within the Resonance and DIS regions [1]–[3].
- Provides data for the continuous investigation of the Quark – Hadron Duality of the nucleons [2], [4], [5].
- Provide a test for LQCD with the second moment measurement from the F2 value of deuterium and the proton [2], [4].

As a step towards attaining the physics goals of this experiment, a study on the Charge Symmetric Background (CSB) contained in the data becomes the key aim of this work. A key objective of this work is to remove the CSB from the HMS 59^o data. This will lead to cross-section measurement and F2 extraction for proton and deuteron.

To achieve the expected outcome of the 59^o data analysis, the work has been divided into four major milestones.

The first is obtaining a working framework, benchmarked by SHMS known results from earlier work. Secondly, is performing a CSB study for the 59^o degree HMS. Thirdly, is to check for other corrections that are needed to be included in the analysis and Finally, obtain the inclusive scattering cross-section and F_2 value.

2 Background

2.1 Introduction

The basic theory for the determination of F_2 for ^1H and ^2H at the DIS and resonance region for a large range of x ($\approx$ 0.2 to 1) and Q^2 ($\approx$ 4 to 16GeV) in an inclusive scattering reaction, is discussed as follows. The reaction involves the scattering of an

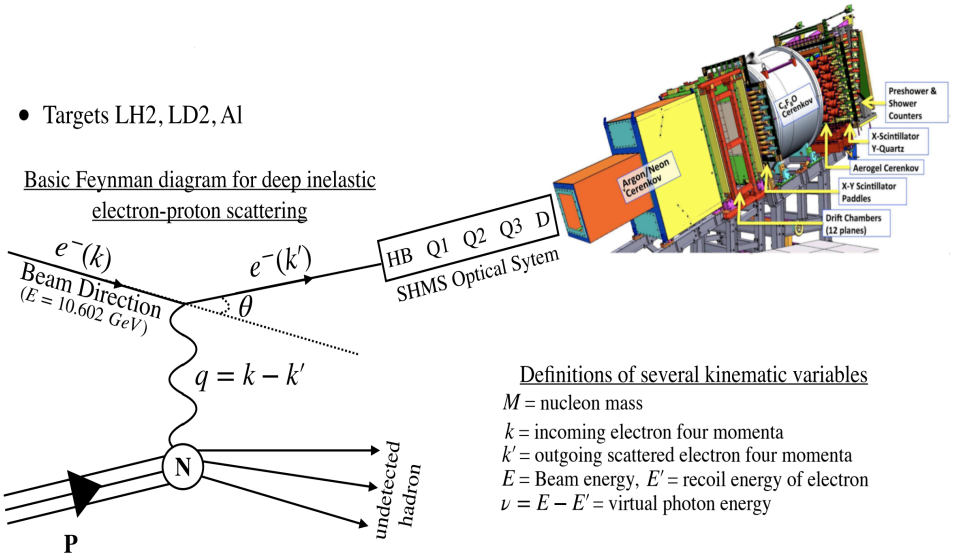

Figure 1 First order Feynman diagram for electron-nucleon inclusive scattering, with SHMS detector collecting data of the scattered electron.

unpolarised electron beam of energy (E = 10.602 GeV), current between 30 and 65μA with momentum k on a 10 cm liquid Hydrogen (LH2) and Deuterium (LD2) target for proton and deuterium F_2 measurement. The electron transfer $q = k - k'$ momentum to the nucleon, and the scattered electron goes with k' momentum and E' energy [6], [7]. The detector tracked the momentum and collect the energy of the scattered electron at the scattering angle θ relative to the incident electron beam.

For the inclusive reaction, the virtual photon energy is $\boldsymbol{\nu = E - E'}$ and the negative squared mass of the virtual photon is $\boldsymbol{-q^2 = Q^2 = 4EE'Sin^2(\frac{\theta}{2})}$. The two quantities have a direct relationship with the measurable quantities obtained from the experiment. The Bjorken scaling parameter is the fraction of the nuclear momentum carried by the struck Parton, and is defined as $\boldsymbol{x_{bj} = \frac{Q^2}{2p.q} = \frac{Q^2}{2M\nu}}$. Similarly, the fraction of the beam energy transferred by virtual photon is given as $\boldsymbol{y = \frac{p.q}{p.k} = \frac{\nu}{E}}$ and the invariant mass squared of the final hadronic state is written as $\boldsymbol{W^2 = (p+q)^2 = M^2 + 2M\nu - Q^2}$. M is the nucleon mass.

2.2 F_2 Nuclear Structure Function

$\boldsymbol{F_2(x, Q^2)}$ is a nuclear structure function. It depends on x, i.e the longitudinal momentum fraction carried by the struct quark, which in this specific case is assumed to be equal to the Bjorken variable $\boldsymbol{x_{bj}}$ (i.e $\boldsymbol{x \sim x_{bj}}$) and square of the momentum transfer $\boldsymbol{Q^2}$ [1], [8]. It is one of the factors in the differential scattering cross-section.

$$\frac{\boldsymbol{d^2\sigma}}{\boldsymbol{d\Omega dE'}} = \frac{\boldsymbol{\alpha^2}}{\boldsymbol{4E^2 sin^4(\frac{\theta}{2})}}[\frac{\boldsymbol{2}}{\boldsymbol{M}}\boldsymbol{F_1(x, Q^2) sin^2(\frac{\theta}{2})} + \frac{\boldsymbol{1}}{\boldsymbol{\nu}}\boldsymbol{F_2(x, Q^2) cos^2(\frac{\theta}{2})}] \tag{2.1}$$

Equation 2.1 is the differential cross-section for the inclusive scattering reaction [9]. It depends on the square of the fine-structure constant α. The two functions F_1 and F_2 parametrize the unknown part of the nuclear structure [10]. In general, F_2 has a higher contribution over F_1.

F_2 can be written in terms of the differential cross-section, the ratio of the longitudinal to transverse photoabsorption cross-section R, the relative longitudinal flux ε, and some $kinematics$ terms. It is given by equation 2.2.

$$\boldsymbol{F_2} = \frac{\boldsymbol{d^2\sigma}}{\boldsymbol{d\Omega dE'}}\frac{\boldsymbol{1+R}}{\boldsymbol{1+\varepsilon R}} * \boldsymbol{Kinematics} \tag{2.2}$$

The $kinematics$ term in eqn. 2.2 is defined in eqn. 2.3 in terms of the flux of transverse virtual photons Γ (eqn. 2.4), with total flux K (eqn. 2.5) and the relative longitudinal flux ε (eqn. 2.7). Each term depends on measurable quantities from the experiment.

$$\boldsymbol{Kinematics} = \frac{\boldsymbol{K\nu}}{\boldsymbol{4\pi^2\alpha}}\frac{\boldsymbol{1}}{\boldsymbol{\Gamma}}\frac{\boldsymbol{1}}{\boldsymbol{1+\frac{\nu^2}{Q^2}}} \tag{2.3}$$

$$\boldsymbol{\Gamma} = \frac{\boldsymbol{\alpha K}}{\boldsymbol{2\pi^2 Q^2}}\frac{\boldsymbol{E'}}{\boldsymbol{E}}\frac{\boldsymbol{1}}{\boldsymbol{1-\varepsilon}} \tag{2.4}$$

$$\boldsymbol{K} = \frac{\boldsymbol{2M\nu - Q^2}}{\boldsymbol{2M}} \tag{2.5}$$

$$\boldsymbol{R} = \frac{\boldsymbol{\sigma_L}}{\boldsymbol{\sigma_T}} \tag{2.6}$$

$$\boldsymbol{\varepsilon} = \boldsymbol{[1 + 2(1 + \frac{Q^2}{4M^2x^2})tan^2(\frac{\theta}{2})]^{-1}} \tag{2.7}$$

The $\boldsymbol{F_2}$ is obtained experimentally from inclusive scattering reactions cross-section measurement as indicated in eqn. 2.2. It has many forms of definition, with one form defined by eqn. 2.2.

3 Analysis

3.1 Introduction

Experiment E12-10-002 was conducted at Jefferson Lab. in the period of February to March 2018. In the experiment, data were obtained with High Momentum Spectrometer(HMS) for lower angles between 21^0 to 39^0 for SuperHMS (SHMS), and for larger angles up to 59^0 HMS was used. The data is from an inclusive nuclear scattering of a 30 to 60μA and 10.602GeV electron beam striking a 10 cm liquid ^{1}H and ^{2}H in an aluminum casing target. The acquired data contain backgrounds. Charge symmetric processes are one of the major contributors to the background. Charge Symmetric Background (CSB) accounted for about 6 to 20% [1] contribution of background in the data. It is higher at higher angles.

3.1.1 Charge Symmetric (CS) Processes

CS processes produce electrons that are indistinguishable from that of the scattered electrons. Neutral Pion Decay is the major source of CSB because within the Q^2 value that we are probing the nucleon, it is favorable for the production of neutral Pions. The neutral Pion have a 98.8% probability of decaying into two gammas. The produced gammas from the decay, subsequently undergo pair production producing electrons and positrons.

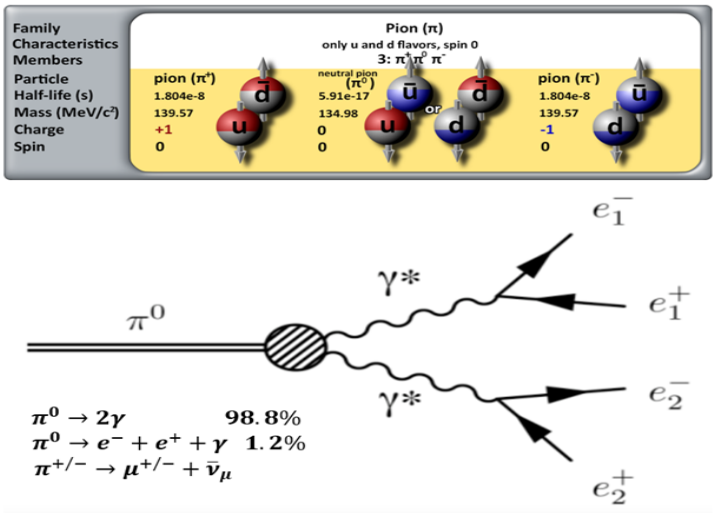

Figure 2 Positive, neutral, and negative Pions constituent quarks. Neutral Pion decay channels and branching ratio.

As seen in Figure 2. The second branch decays directly to positron, electron, and gamma. The process is charge symmetric because the number of electrons and positrons produced in the process is the same.

3.2 CSB Analysis

Exclusive scattering experiments have the advantage that the setup can be made to eliminate a large number of background electrons by performing a coincidence between the scattered electron and the struck nucleon. This procedure is not obtainable in the inclusive experiment, as only the scattered electrons are detected in the experiment. However, the CS process is charge symmetric. Implying that by measuring the positron counts, the number of electrons produced in the process can be obtained. The positron yield for the experiment is measured by changing the polarity of the spectrometer magnet with the same kinematic settings as that of the electrons. From the whole electron yield (e-) with the same kinematics, the positron yield (e+) to scattered electron yield ratio $\frac{e^+}{e^- - e^+}$ is then obtained.

3.3 $\frac{e^+}{e^- - e^+}$ Extraction From the Data

The computation involves the choice of the input variables. The input variables are based on the results one is interested in checking. The inputs are the target, Spectrometer angle, type of spectrometer, and the central momentum value.

The data from each run of the experiment is used. The collected data is Y_{exp}. It is corrected event by event to obtain Y_{corrd}. The weighting used for this correction is $\boldsymbol{PC_\pi/(\varepsilon_{track} * \varepsilon_{trig} * biol * C_{LT})}$

$$\boldsymbol{Y_{corrd} = \frac{Y_{exp} * PC_\pi}{\varepsilon_{track} * \varepsilon_{trig} * biol * C_{LT}}} \tag{3.1}$$

Equation 3.1 gives the result Y_{corrd} of the first correction applied to experimental data Y_{exp}, computed event by event. PC_π is the pion contamination, ε_{track} is the tracking efficiency, ε_{trig} is the triggering efficiency, $biol$ is the boiling correction due to the heating of the liquid target and C_{LT} is the computer live time.

$$\boldsymbol{Y_{Corrd} = Y_{corrd} * PS} \tag{3.2}$$

At the end of every run, Y_{Corrd} yield is obtained by multiplying Y_{corrd} with the pre-scale (PS) value. As seen in equation 3.2.

$$\boldsymbol{Y_{Charged\_Norm.} = \frac{Y_{Corrd}}{Charge_{tot.}}} \tag{3.3}$$

Furthermore, at the end of every run for a particular kinematic setting and for positron or electron specie, the whole charge for that run is collected and added together for the whole available runs of such settings to obtain $Charge_{tot.}$. The charge normalized yield $\boldsymbol{Y_{Charged\_Norm.}}$ is then obtained by dividing Y_{Corrd} with $Charge_{tot.}$ as given in equation 3.3. Figures 3 and 4 give two examples of the charged normalized yield for hydrogen target with central momentum of 1.966 GeV, for SHMS spectrometer angle of 29^0 for positron and electron respectively.

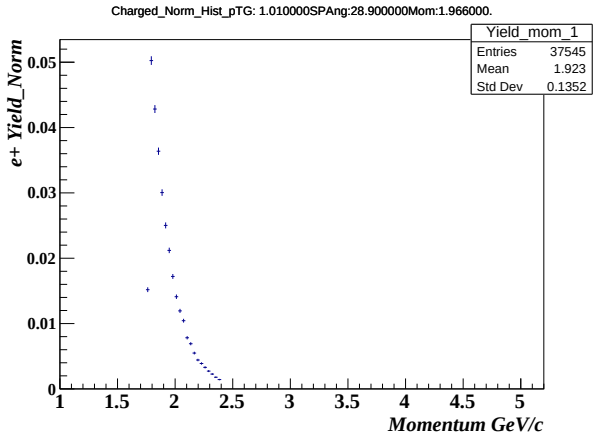

Figure 3 Positron Charged Normalized Yield for Hydrogen at 29^0.

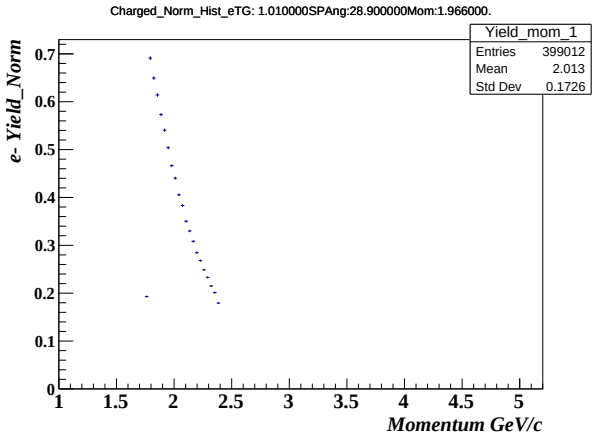

Figure 4 Electron Charged Normalized Yield for Hydrogen at 29^0.

The $\frac{e^+}{e^- - e^+}$ is obtained by taking the ratio of the positron histograms to the electron minus positron histograms as stated in equation 3.4

$$\frac{\boldsymbol{e^+}}{\boldsymbol{e^- - e^+}} = \frac{\boldsymbol{Y_{Charged\_Norm.\_e+}}}{\boldsymbol{Y_{Charged\_Norm.\_e^-} - Y_{Charged\_Norm.\_e+}}} \tag{3.4}$$

Equation 3.4 gives the ratio of the positron in the data to the number of scattered electrons detected. The amount of scattered electrons from the total electrons detected is $e^- - e^+ = Y_{Charged\_Norm.\_e^-} - Y_{Charged\_Norm.\_e+}$.

3.4 Corrections on Data

The amount of individual corrections seen in the $\frac{e^+}{e^- - e^+}$ yield is calculated using eqn 3.5.

$$\boldsymbol{Y_{corrd}} = \frac{\boldsymbol{Y_{exp}}}{\boldsymbol{C_{LT}}}, = \frac{\boldsymbol{Y_{exp}}}{\boldsymbol{\varepsilon_{track}}}, = \frac{\boldsymbol{Y_{exp}}}{\boldsymbol{\varepsilon_{trig}}}, = \frac{\boldsymbol{Y_{exp}}}{\boldsymbol{biol}}, = \boldsymbol{Y_{exp} * PC_{\pi}} \tag{3.5}$$

An example is seen in figure 5. One can see that the Computer livetime has the largest contribution in increasing the $\frac{e^+}{e^- - e^+}$ yield relative to the other corrections. On the other hand, the pion contamination lowers the $\frac{e^+}{e^- - e^+}$ yield. A further correction check was

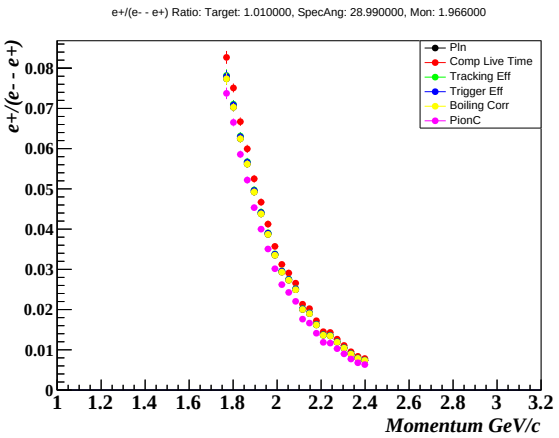

Figure 5 Histogram of $\frac{e^+}{e^- - e^+}$: corrections placed separately to visualize their effects.

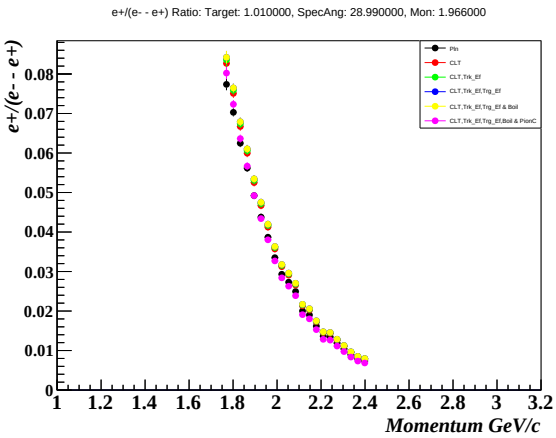

Figure 6 Histogram of $\frac{e^+}{e^- - e^+}$: corrections added sequentially to visualize their effects.

performed to see the total contributions added sequentially. Equations 3.6 to 3.10 were used respectively. An example of such a plot is in figure 6. One can generally see that the corrections sequentially increased the $\frac{e^+}{e^- - e^+}$ yield. While the pion contamination lowers the $\frac{e^+}{e^- - e^+}$ yield below the plain one at larger momentum and just above the plain one at lower momentum. In general, the corrections are less at higher momentum and more at lower momentum.

$$Y_{corrd} = \frac{Y_{exp}}{C_{LT}} \tag{3.6}$$

$$Y_{corrd} = \frac{Y_{exp}}{C_{LT} * \varepsilon_{track}} \tag{3.7}$$

$$Y_{corrd} = \frac{Y_{exp}}{C_{LT} * \varepsilon_{track} * \varepsilon_{trig}} \tag{3.8}$$

$$Y_{corrd} = \frac{Y_{exp}}{C_{LT} * \varepsilon_{track} * \varepsilon_{trig} * biol} \tag{3.9}$$

$$Y_{corrd} = \frac{Y_{exp} * PC_{\pi}}{C_{LT} * \varepsilon_{track} * \varepsilon_{trig} * biol} \tag{3.10}$$

3.5 $\frac{e^+}{e^- - e^+}$ for SHMS Data

The $\frac{e^+}{e^- - e^+}$ was obtained for different angles (39^0,29^0,21^0) and targets (H, D). The result is seen in figure 7.

Figure 7 includes all the kinematics settings that were taken with SHMS during the experiment that contain positron data. The result indicates that the CSB contribution is low at smaller angles and higher momentum than at larger angles and smaller momentum.

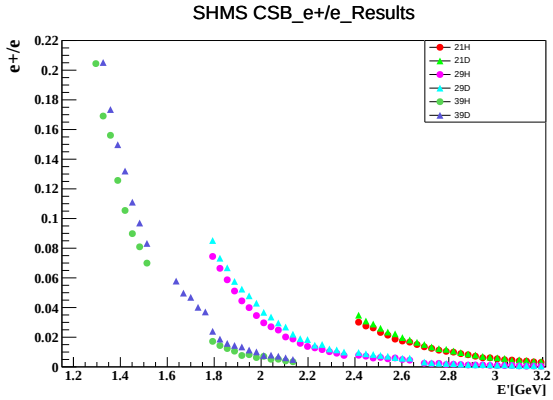

Figure 7 Plot of $\frac{e^+}{e^- - e^+}$ as a function of scattered electron energy for different angles. It's more at higher angles

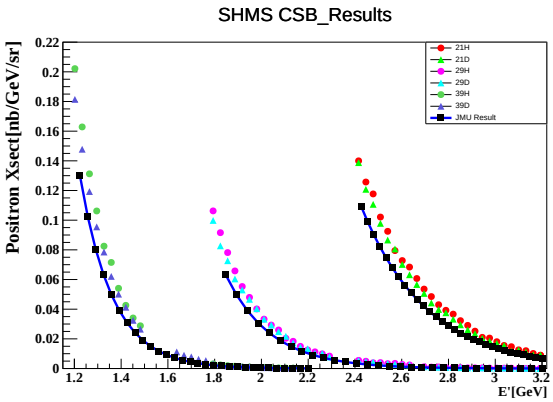

Figure 8 Positron cross-section. Compared with results from James Madison University (JMU)

To be able to estimate the number of positrons in the data where the positron runs were not taken during the experiment, a method was developed that involves obtaining a relationship between two parametrized values obtained from the positron differential cross-section. The positron cross-section is obtained from the product of the measured electron radiative corrected differential cross-section $\frac{d^2\sigma_{e^-}}{d\Omega dE'}$ with the $\frac{e^+}{e^- - e^+}$ yield, as given in equation 3.11.

$$\frac{d^2\sigma_{e^+}}{d\Omega dE'} = \left(\frac{Y_{e^+}}{Y_{e^-} - Y_{e^+}}\right)\frac{d^2\sigma_{e^-}}{d\Omega dE'} \tag{3.11}$$

Figure 8 is the positron cross-section, obtained from the data as a function of the scattered electron energy. The result is in agreement with earlier results from JMU with the black square markers.

The results in figure 8 were fitted with the parametrized positron differential cross-section of equation 3.12.

$$\frac{d^2\sigma_{e^+}}{d\Omega dE'} = e^{p_0}\left(e^{p_1(E_b - E')} - 1\right) \tag{3.12}$$

The parametrized positron differential cross-section $\frac{d^2\sigma_{e^+}}{d\Omega dE'}$ is parametrized in terms of E_b, E' which are the beam and scattered e^- energy and the parameters p_0, p_1. $p_0(\theta), p_1(\theta)$ are used to calculate this effect at other angles (θ = 25^0, 33^0), where e^+ data were not taken due to time constrain.

Figure 9 is contained the values of the fitting performed using equation 3.12. It also contained the result of the relative percentage error from this fitting to those obtained from JMU. The relative percentage error is obtained using equation 3.13. Where P_i is

	P0	P0 error	P1	P1 erro	P0 JMU	P1 JMU	% Error P0	% Error P1
H21	-31.28	0.087	3.58	0.011	-31.4	3.57	0.3821656051	0.2801120448
D21	-31.31	0.048	3.58	0.006	-31.4	3.57	0.2866242038	0.2801120448
H29	-48.08	0.052	5.2	0.006	-48.2	5.19	0.2489626556	0.1926782274
D29	-48.11	0.084	5.2	0.009	-48.2	5.19	0.1867219917	0.1926782274
H39	-68.85	0.065	7.16	0.007	-69	7.14	0.2173913043	0.2801120448
D39	-68.9	0.084	7.15	0.009	-69	7.14	0.1449275362	0.1400560224

Figure 9 Positron cross-section fitting parameters values with the relative % error

the fitting parameter from this work and $P_{i,JMU}$ is that from JMU. i is either 0 for the first parameter or 1 for the second parameter.

$$\%Error = \mid \frac{P_i - P_{i,JMU}}{P_{i,JMU}} \mid *100 \tag{3.13}$$

Figure 10 is the relative percentage of errors for the fitting parameters value represented in a bar chart. One sees that the relative errors are less than 0.4%.

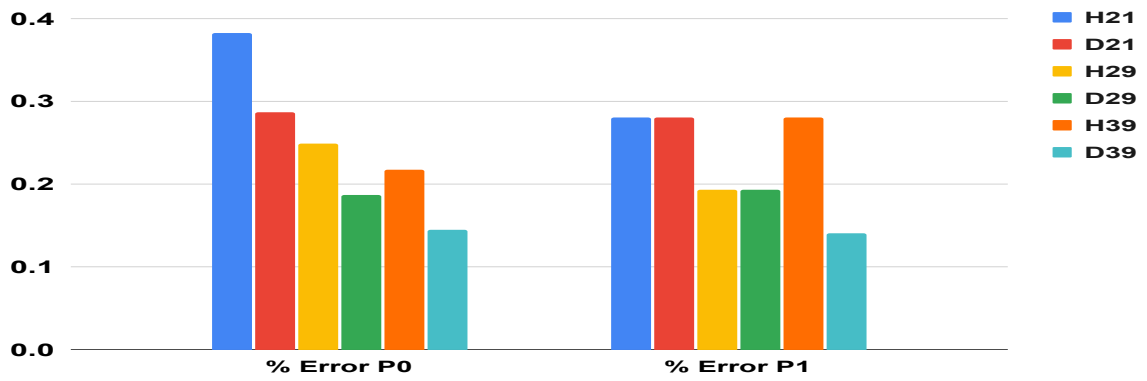

Figure 10 Percentage error of fitting parameters relative to that from JMU

The fitting is consistent with the results obtained by JMU. The largest fitting error is seen at the smallest angle of 21^0 of about 0.38%. The CSB is similar for both types of targets.

4 Conclusion

4.1 Conclusion

SHMS Charge symmetric background has been analyzed. It was compared with results earlier obtained by JMU for the spectrometer angles of 21^0, 29^0, and 39^0 each with two targets (^{1}H and ^{2}H). The results for the spectrometer angle of 39^0 indicate the largest Charge Symmetric background contribution. While the largest fitting error of 0.38% is at 21^0. The results imply that a framework has been developed that can be used for other angles analysis, where the positron data was not taken. And can easily be adapted for the HMS detector data analysis.

4.2 Future work

This work implies that a framework has been developed and can be used for further data analysis. The framework will be used to analyze the HMS data for a spectrometer angle of 59^0. The 59^0 data analysis is significant [9] because it is where the Q^2 is the largest, with the CSB contribution expected to be high. It also has the smallest contribution to the cross-section.

References

[1] S. Malace, M. Paolone, S. Strauch, *et al.*, “Precision measurements of the f2 structure function at large x in the resonance region and beyond”,

[2] S. Malace. “5th international workshop on nucleon structure at large bjorken x”. (2019), [Online]. Available: https://indico.cern.ch/event/799284/contributions/3478960/attachments/1894433/3125081/malace_hix2019.pdf.

[3] A. Karki, *Precise measurement of the nuclear dependence of the EMC effect in light nuclei*. Mississippi State University, 2022.

[4] I. Albayrak, V. Mamyan, M. Christy, *et al.*, “Measurements of nonsinglet moments of the nucleon structure functions and comparison to predictions from lattice qcd for q 2= 4 gev 2”, *Physical review letters*, vol. 123, no. 2, p. 022 501, 2019.

[5] A. Sun, “Measurement of h (e, e’) and d (e, e’) cross-sections for bloom-gilman quark-hadron duality study”, Tech. Rep., 2022.

[6] P. B. Pal, *An introductory course of particle physics*. Taylor & Francis, 2014.

[7] B. Povh, K. Rith, C. Scholz, F. Zetsche, and W. Rodejohann, “Particles and nuclei”, *An Introduction to the Physical Concepts, Berlin and Heidelberg: Springer-Verlag (Italian Translation:(1998), Particelle e nuclei. Un’introduzione ai concetti sici, Torino: Bollati Boringhieri editore)*, 1995.

[8] D. Biswas, “Extraction of proton and deuteron f 2 structure function from inclusive electron-nucleon scattering at large bjorken- x”, Ph.D. dissertation, Hampton University, 2022.

[9] H. Williams. “Symposium: Nucleon and nuclei structure from inclusive measurements”. (2023), [Online]. Available: https://indico.phys.vt.edu/event/60/contributions/1195/attachments/925/1290/inclusiveWorkshop2023.pdf.

[10] F. Halzen, A. Martin, and L. Quarks, “An introductory course in modern particle physics”, *John and Wiley*, 1984.